Published in final edited form as:
Hippocampus. 2011 January ; 21(1): 81–92. doi:10.1002/hipo.20725.

Phosphacan and Receptor Protein Tyrosine Phosphatase β Expression Mediates Deafferentation-Induced Synaptogenesis

Janna L. Harris, **Thomas M. Reeves**, and **Linda L. Phillips**
Department of Anatomy and Neurobiology, School of Medicine, Virginia Commonwealth University Medical Center, Richmond, VA 23298

Abstract

This study documents the spatial and temporal expression of three structurally related chondroitin sulfated proteoglycans (CSPGs) during synaptic regeneration induced by brain injury. Using the unilateral entorhinal cortex lesion model of adaptive synaptogenesis, we documented mRNA and protein profiles of phosphacan and its two splice variants, full length receptor protein tyrosine phosphatase β (RPTPβ) and the short transmembrane receptor form (sRPTPβ), at 2, 7, and 15 d postlesion. We report that whole hippocampal sRPTPβ protein and mRNA are persistently elevated over the first two weeks after UEC. As predicted, this transmembrane family member was localized adjacent to synaptic sites in the deafferented neuropil and showed increased distribution over that zone following lesion. By contrast, whole hippocampal phosphacan protein was not elevated with deafferentation, however, its mRNA was increased during the period of sprouting and synapse formation (7d). When the zone of synaptic reorganization was sampled using molecular layer/granule cell (ML/GCL) enriched dissections, we observed an increase in phosphacan protein at 7d, concurrent with the observed hippocampal mRNA elevation. Immunohistochemistry also showed a shift in phosphacan distribution from granule cell bodies to the deafferented ML at 2 and 7d postlesion. Phosphacan and sRPTPβ were not co-localized with glial fibrillary acid protein (GFAP), suggesting that reactive astrocytes were not a major source of either proteoglycan. While transcript for the developmentally prominent full length RPTPβ was also increased at 2 and 15d, its protein was not detected in our adult samples. These results indicate that phosphacan and RPTPβ splice variants participate in both the acute degenerative and long-term regenerative phases of reactive synaptogenesis. These results suggest that increase in the transmembrane sRPTPβ tyrosine phosphatase activity is critical to this plasticity, and that local elevation of extracellular phosphacan influences dendritic organization during synaptogenesis.

Keywords

entorhinal lesion; synaptic plasticity; proteoglycan; dentate gyrus; gene expression

Introduction

Functional recovery after traumatic brain injury requires axonal sprouting and synaptic reorganization. There is increasing evidence that these processes are regulated by molecules within the extracellular environment of the brain. The brain extracellular matrix (ECM) is enriched in proteoglycans, particularly CSPGs. As a group, CSPGs were initially thought to inhibit axon growth and plasticity both *in vitro* and *in vivo* (Snow et al., 1990; Oohira et al., 1991; Grumet et al., 1993; Davies et al., 1999). They are also major components of the

Corresponding Author: Dr. Linda L. Phillips, Department of Anatomy and Neurobiology, PO Box 980709, School of Medicine, Virginia Commonwealth University Medical Center, Richmond, VA 23298, (804)828-9657, llphilli@vcu.edu.

inhibitory glial scar which forms after lesions to the brain or spinal cord (reviewed in Properzi et al., 2003). Published evidence shows that enzymes which degrade chondroitin sulfated-glycosaminoglycans (GAGs) may enhance axon regeneration and synaptic plasticity (Moon et al., 2001; Bradbury et al., 2002; Pizzorusso et al., 2002; Huang et al., 2006). More recently, focal cortical contusion was reported to differentially affect CSPG expression and reduce inhibitory proteoglycans in regions bordering the lesion core, potentially fostering local plasticity (Harris NG et al., 2009). By contrast, some CSPG family members are elevated after brain injury and appear to interact in a positive way with cell adhesion molecules and soluble growth factors to enhance axonal sprouting (Faissner et al., 1994; Sakurai et al., 1997; Bicknese et al., 1994; Schafer et al., 2008). Together, these data show that CSPG interactions may be complex, potentially both inhibitory and supportive of regenerative plasticity. The CSPG phosphacan and its related splice variants are one proteoglycan group whose members may play a supportive role in the neuronal plasticity processes.

Phosphacan (6B4 proteoglycan, or DSD-1 proteoglycan in the mouse) is a secreted alternative splice variant of the full length receptor protein tyrosine phosphatase β (RPTPβ), a transmembrane receptor with intracellular tyrosine phosphatase activity (Maurel et al., 1994). A third form, the short receptor form sRPTPβ, lacks the extracellular membrane-proximal sequence but retains the intracellular phosphatase activity. Secreted phosphacan and transmembrane sRPTPβ are the two most prominent forms found in adult brain (Sakurai et al., 1996; Dobbertin et al., 2003). Produced by both neurons and glia (Snyder et al., 1996; Hayashi et al., 2005), phosphacan is a major component of brain matrix and can inhibit or promote axon growth, depending on the neuronal lineage (Garwood et al., 1999). This splice variant is secreted into the ECM and is distributed around synaptic junctions, but absent from the synaptic active zone (Miyata et al., 2004). Relative to other CSPGs (e.g. neurocan, versican, NG2) which may be up-regulated after CNS trauma (Asher et al., 2000; Asher et al., 2002; Morgenstern et al., 2002; Jones et al., 2003; Schafer et al., 2008), phosphacan may vary significantly after injury. For example, it is reduced following spinal cord injury (Jones et al., 2003; Tang et al., 2003), cortical stab injury (Dobbertin et al., 2003) and filter implant-induced glial scarring (McKeon et al., 1999). However, others report increased phosphacan after experimental stroke (Carmichael et al., 2005) and fimbria/fornix lesion (Snyder et al., 1996). While one recent study (Schafer et al., 2008) reported no change in phosphacan mRNA expression after entorhinal deafferentation lesion, a systematic analysis of phosphacan splice variants during reactive synaptogenesis has not been made.

Ultrastructural studies confirm that membrane-type full length RPTPβ and sRPTPβ expression are associated with post-synaptic dendrites and spines (Hayashi et al., 2005). Other reports suggest a role for RPTPβ in the production of long term potentiation (LTP) within the mature brain, a function which is consistent with synaptic localization. RPTPβ knockout mice display age-dependent abnormalities in hippocampal LTP, as well as impaired spatial learning and contextual fear conditioning (Niisato et al., 2005; Tamura et al., 2006). A number of intracellular targets for RPTPβ phosphatase have been identified (Kawachi et al., 1999; Meng et al., 2000; Pariser et al., 2005; Tamura et al., 2006), many of which direct neurite morphogenesis and synapse regeneration or stabilization (e.g. β-catenin, β-adducin, PSD-95, p190 RhoGAP). Together, these results suggest that RPTPβ can influence synaptic plasticity, possibly through multiple molecular pathways.

Clearly, expression of CSPGs like phosphacan and RPTPβ is altered with CNS trauma and may act to regulate the subsequent axonal sprouting and synaptic recovery. In the present study we document the spatial and temporal expression of phosphacan, RPTPβ and sRPTPβ during synaptic reorganization induced by unilateral entorhinal cortex lesion (UEC). UEC is a well-characterized rodent model of synaptic plasticity (Steward et al., 1988), generating

robust synaptogenesis within the dentate gyrus during the first two weeks post-lesion. This time course permits examination of mRNA and protein for the different phosphacan splice variants during periods of terminal degeneration (2d), afferent sprouting and synapse formation (7d) and synapse stabilization (15d). We report differential mRNA and protein expression for phosphacan and RPTPβ splice variants over the first two weeks postinjury, supporting a role for these CSPGs in both the degenerative and regenerative phases of reactive synaptogenesis.

Materials and Methods

Experimental Animals

Adult male Sprague-Dawley rats (300–390g) were used in this study. Rats were randomly divided into three experimental groups: 2d (n = 17), 7d (n = 23) and 15d (n = 12) survival. Rats were housed in pairs within individual cages having food and water *ad libitum*, and subjected to a 12hr dark-light cycle at 22°C. All protocols for injury and use of animals were approved by the Institutional Animal Care and Use Committee of Virginia Commonwealth University.

Unilateral Entorhinal Cortex Lesion (UEC)

Rats were subjected to UEC after the method of Loesche and Steward (1977). All animals were surgically prepared under isoflurane anesthesia delivered via nose cone (2% in carrier gas of 70% N_2O, 30% O_2). During all surgical procedures, body temperature was maintained at 37°C via a thermostatically controlled heating pad (Harvard Apparatus). Rats were placed in a stereotaxic frame, and an area of skull was removed above the entorhinal cortex of the right hemisphere. Lesion current was passed through a Teflon-insulated wire electrode angled at 10° from vertical. Current was delivered (1.5 mA for 30 sec) at a total of nine stereotaxic sites: 1.5 mm anterior to the transverse sinus, 3, 4 and 5 mm lateral to midline; and at 2, 4 and 6mm ventral to the brain surface. After lesions were completed, the electrode was removed, the scalp was sutured closed over the surgical site and Bacitracin applied to the wound. Animals were monitored during full recovery from anesthesia and returned to their home cages.

Protein Extraction and Western Blotting

Two rapid dissection procedures for ipsilateral and contralateral samples were performed. Whole hippocampi were removed from one subset of animals at 2d (n =5), 7d (n = 9), or 15d (n = 6) post-lesion, and a dentate molecular layer enriched fraction was removed from a second subset of rats at 2d (n = 3) and 7d (n = 4) post-lesion. For the whole hippocampal tissue, a serial extraction protocol was adapted from Dobbertin et al. (2003) in order to separate soluble extracellular phosphacan from transmembrane RPTPβ and sRPTPβ. Each hippocampus was homogenized in 1.75 ml detergent-free extraction buffer (50mM Tris, 150mM NaCl, 40mM Na Acetate) containing protease inhibitors (Roche complete cocktail plus 2μg/ml Pepstatin). Homogenates were centrifuged for 20 min at 100,000 × *g* and 4°C. Supernatant was removed and stored at −80°C as the saline soluble fraction. Pellets were re-homogenized in 1.75ml extraction buffer containing 1% Triton X-100, and agitated for 1 h at 4°C prior to centrifugation for 20 min at 100,000 × *g* and 4°C. Supernatant was removed and stored at −80°C as the detergent soluble fraction. In order to expose antigenic sites and maximize efficiency of antibody recognition, all protein samples were treated with chondroitinase ABC (chABC; Seikagaku America) to remove chondroitin sulfate GAG chains from proteoglycans. Aliquots of 540 μl for each sample were removed, buffered to pH 8 by addition of 400 mM Tris, and mixed with an additional protease inhibitor (Roche complete cocktail plus 2μg/ml Pepstatin). The resulting preparation (600μl volume) was incubated with 0.3 U chABC for 3 h, shaking at 37°C. Reaction was stopped by returning

samples to −80°C. Protein concentration was determined in aliquots from the treated samples using spectrophotometry (Shimadzu UV-160; Shimadzu Scientific Instruments).

For blot preparation, samples were heat denatured in XT sample buffer (Bio-Rad Laboratories), either 5μg (phosphacan probe) or 18μg (RPTPβ probe) separated on 3–8% gels (Bio-Rad Laboratories, Hercules, CA) before transfer to PVDF membrane. Membranes were blocked in 5% milk-TBST (Tris buffered saline containing 0.05% Tween 20) for 1h before being probed with either mouse phosphacan (3F8; Developmental Studies Hybridoma Bank, University of Iowa) or mouse RPTPβ (BD Biosciences, San Jose, CA) antibody diluted in milk-TBST (1.5 μg/mL) overnight at 4°C. This RPTPβ antibody targets the c terminus common to both short and full length proteins (Levy et al., 1993), thereby recognizing each RPTPβ isoform. Blots were subsequently washed with milk-TBST and then incubated for 1h at room temperature in peroxidase conjugated goat anti-mouse secondary antibody (1:20,000; Rockland; Gilbertsville, PA) prior to a final washing in TBST and immunopositive signal visualization using Super Signal West Dura Extended Duration Substrate (Thermo Scientific; Rockford, IL). Parallel blots were incubated without primary antibody to confirm signal specificity. All blots were then imaged digitally with the G:Box ChemiHR system for densitometric analysis using GeneSnap software (SynGene; Frederick, MD). In each case, the ipsilateral densitometric measurements were expressed as a percent of contralateral value.

The second subset of animals at 2d (n = 3) and 7d (n = 4) postlesion were prepared for enriched molecular layer extraction. Using coronal tissue blocks, the dentate molecular layer and a portion of the adjacent granule cell lamina were excised, homogenized in a 100μl volume of TPER (Thermo Scientific) and centrifuged for 5 min at 8,000×*g* and 4°C. Supernatant was removed and stored at −80°C. As for whole hippocampal protein extracts, 5μg of protein was separated on Criterion XT 3–8% gels and transferred to PVDF membrane prior to probing for phosphacan using the 3F8 antibody. Immunopositive bands were visualized, digitally imaged and densitometrically analyzed as described above for whole hippocampal blots.

After primary antibody binding data was captured, all blots were stripped and reprobed for β-actin (mouse monoclonal, Sigma, St. Louis, MO; 1:3000) as a load control. Signal was visualized as described above for the 3F8 and RPTPβ antibodies and blots imaged with the same G:Box ChemiHR system. No quantitative differences in load between the lanes were detected.

Confocal Immunohistochemistry

At 2d (n = 3) or 7d (n = 3) post-lesion, groups of rats were deeply anesthetized with sodium pentobarbital (60 mg/kg, i.p.) and sacrificed by transcardiac perfusion of 0.9% saline, followed by 4% formaldehyde in 0.1M phosphate buffer (PB), pH 7.2. Brains were removed and post-fixed overnight at 4°C. Coronal sections (40 μm) were collected in 0.1 M PB, and immunohistochemistry (IHC) was performed for phosphacan and RPTPβ using the same antibodies described above for Western blotting. In some sections, 3F8 or anti- RPTPβ was applied in combination with rabbit antibody to GFAP (Dako North America Inc., Westbury, NY) to determine if astrocytes were a possible source of phosphacan or RPTPβ. Similarly, anti-RPTPβ was used in co-localization experiments with rabbit postsynaptic density-95 (PSD-95) antibody (Zymed Laboratories, San Francisco, CA) to probe for association between the membrane receptor form and synaptic junctions. Since the binding site for 3F8 is partially masked by GAGs attached to the core protein (Dobbertin et al. 2003), we treated brain sections with chABC prior to phosphacan immunodetection. These sections were incubated for 1 h at 37°C with chABC (0.1 U/mL in Tris Acetate buffer; 100 mM Tris-HCl, 30 mM Na-Acetate, pH 8.0), then washed 3 × 10 min in phosphate buffered saline (PBS;

Bio-Rad Laboratories, Hercules, CA) before subsequent immunodetection. Free-floating sections were then blocked for 30 min in peroxidase, washed 3 × 10 min in PBS and placed in blocking buffer (fish gelatin in PBS + 0.05% Triton X-100) for 30 min. Next, the tissue sections were incubated in primary antibody (3F8, anti-phosphacan 1:100, anti-RPTPβ 1:500, anti-GFAP 1:5,000, anti-PSD-95 1:500), in paired combinations overnight at 4°C. After primary antibody exposure, sections were washed 3 × 10 min in PBS, blocked again for 30 min and incubated with the appropriate fluorescent secondary antibodies (Alexa 488 goat-anti-mouse, or Alexa 594 donkey anti-rabbit; Invitrogen, Carlsbad, CA) for 2 h. After a final series of PBS washes, sections were mounted onto Probe On Plus glass slides (Fisher Scientific, Pittsburgh, PA), and coverslipped with Vectashield (Vector Laboratories, Burlingame, CA). Minus primary controls were processed in parallel to confirm signal specificity. Images were captured with a Leica TCS-SP2 confocal microscope for qualitative analysis of protein distribution.

EM Ultrastructural Immunocytochemistry

At 7d, a subset of animals (n=2) were deeply anesthetized with sodium pentobarbital (60 mg/kg, i.p.) and sacrificed by transcardiac perfusion of 0.9% saline, followed by mixed aldehyde fixative (4% paraformaldehyde and 0.2% glutaraldehyde) in 0.1M PB, pH 7.2. Brains were removed and post-fixed overnight at 4°C. Coronal sections (40 μm) were collected in 0.1 M PB and processed for immunocytochemistry (ICC) with anti-RPTPβ antibody (BD Biosciences, San Jose, CA) as indicated above, or with mouse MAB 5210 antibody (Chemicon/Millipore, Billerica, MA) to detect all phosphacan splice variants. Antibody binding was visualized with DAB as described previously (Phillips et al., 1994). Tissue was then placed in 1% osmium (0.1M phosphate buffer, pH 7.2) and processed in resin prior to being flat-embedded on plastic slides. After the plastic had cured, sample regions of mid-dorsal hippocampus containing the CA1 and dentate gyrus were excised and a series of thick and thin sections cut on an Leica EM UC6i ultramicrotome (Leica Microsystems, Wetzlar, Germany). The thin sections were collected on membrane-coated slotted grids and observed on a Jeol JEM-1230 electron microscope equipped with a Gatan UltraScan 4000SP CCD camera. The granule cell and molecular layers of the dentate gyrus, both ipsilateral and contralateral to the lesion, were systematically photographed at 5–10,000× magnification for qualitative analysis.

RNA Isolation and qRT-PCR

Whole hippocampi were rapidly dissected from a subset of animals at 2d (n = 6), 7d (n = 5), or 15d (n = 6) post-lesion and RNA extraction was performed under nuclease-free conditions. Each hippocampus (~100mg) was homogenized in 1ml Trizol Reagent (Invitrogen, Carlsbad, CA), mixed with 0.2 ml chloroform, and centrifuged for 15 min at 12,000 × *g*. RNA in the upper phase was removed and precipitated with 0.5 ml isopropyl alcohol. After centrifugation for 10 min at 12,000 × *g*, supernatant was removed and RNA pellets were washed in 75% ethanol. The pellets were dissolved in PCR-grade water (Ambion) and incubated at 55°C for 10 min. All samples were then given two cycles of DNAse treatment to remove residual DNA contamination using the DNA-free DNase kit (Ambion; Austin, TX), according to the manufacturer's protocol. Briefly, samples were incubated in a mixture of DNAse buffer and DNAse 1 for 20 min at 37°C, followed by 10 min at room temperature with DNAse Inactivation Reagent. After centrifugation at 10,000 × g for 2 min to pellet inactivation reagent, supernatants were removed and stored at −80°C.

RNA concentration and integrity were first assessed for all samples with the Experion automated electrophoresis system (Bio-Rad Laboratories; Hercules, CA), after which concentration was verified by NanoDrop spectrophotometry (ND-1000, NanoDrop Products; Wilmington, DE). Subsequent electropherogram analysis (Agilent Technologies; Santa

Clara, CA) indicated high quality RNA (RIN ≥7.0), clear peaks for 18S and 28S rRNA and minimal sample degradation. Total RNA was prepared for each sample in PCR-grade water (20 ng/μl) and submitted for TaqMan One-Step RT-PCR on the ABI prism 7900 Sequence Detection system (Applied Biosystems; Foster City, CA). Specific TaqMan primers were designed to span exon-exon boundaries using Primer Express software (Applied Biosystems; Foster City, CA). Sequences for specific primers and TaqMan probes are listed in Table 1. A reference calibrator sample of total RNA was serially diluted and used to generate a standard Cycle Threshold (C_T) vs. Quantity plot for each run. In all cases, the plot was linear and the correlation coefficients were greater than 0.98. PCR reactions were performed in triplicate and relative mRNA quantity was determined as a function of the C_T for each test sample. By this standard curve method, change in target RNA was expressed in arbitrary units relative to the standard calibrator. These units were used for RNA data analysis and were plotted as relative RNA Quantity. Reactions had an overall efficiency between 90–100% as determined by the slope of the standard curves (range −3.1 to −4.2), calculated as $E=10^{(-1/\text{slope})}-1$. Negative controls on each plate included no-amplification and no-template conditions.

Statistical Analysis

Changes in gene and protein expression following UEC were evaluated by comparison of ipsilateral deafferented samples to those from the uninjured contralateral hemisphere, providing within-subject matched controls. Results were expressed as percent of control value. The significance of UEC-induced changes in RNA levels was evaluated using mixed-design ANOVA (SPSS v11, MANOVA) with survival interval as between-subjects factor and hemisphere as within-subjects factor, and evaluations at single survival intervals implemented as a-priori comparisons using simple main effects (Keppel, 1991; Levine, 1991). The normality of sample data distributions was confirmed with normal probability plots prior to ANOVA analyses. The significance of densitometric values from Western blots was analyzed using the Student's t-test. A probability of less than 0.05 was considered statistically significant for all tests.

Results

Expression of Phosphacan and RPTPβ Protein After UEC

Phosphacan protein expression was examined in the saline fraction of hippocampal homogenates extracted without detergent and treated with chABC. A 450 kD phosphacan band was resolved (Figure 1 A), corresponding to the profile of this splice variant reported by Dobbertin et al. (2003). Overall, we found no significant change in phosphacan protein at the three postinjury intervals. By contrast, when hippocampal homogenates extracted with detergent and chABC treated were probed for total RPTPβ, we observed significant increase in the 250 kD band corresponding to sRPTPβ (Dobbertin et al., 2003) at 2, 7, and 15d after UEC (Figure 1B; 116.6 ± 8.2%, $p<0.05$; 118.4 ± 9.5% and 120.2 ± 10.4%, $p<0.001$). By contrast, we failed to detect measurable full length RPTPβ in our Western blot samples, consistent with the reported very low levels of this splice variant in adult tissue (Sakurai et al. 1996; Dobbertin et al 2003). Re-probe of all blots for β-actin verified equal lane loading. These results show that UEC lesion differentially affects expression of the phosphacan and sRPTPβ isoforms.

Phosphacan and RPTPβ Immunohistochemistry

In order to confirm tissue distribution of phosphacan and sRPTPβ, we examined the cellular localization of these proteoglycans using the same antibodies applied for the Western blot experiments. Confocal IHC analysis revealed prominent ipsilateral differences in expression at 2 and 7d postlesion for phosphacan. The greatest change occurred at 2d (Figure 2 A, B),

with diffuse low level staining for phosphacan evident in the contralateral molecular layer (ML), and dense aggregates of the protein surrounding the cell bodies of dentate granule cells (**arrows in** Figure 2A) and within the hilar subgranular zone (**SGZ in** Figure 2 A). By contrast, increased phosphacan immunoreactivity was seen over the outer ML ipsilateral to UEC lesion (**arrows in** Figure 2 B). Notably, the strong phosphacan staining within both granule cells and the subgranular zone was reduced on the deafferented side (Figure 2 B). This result would be consistent with the absence of change in total extracted phosphacan after injury but indicates a clear lesion-induced shift in the cellular distribution of the protein.

While Western blot results showed an increase of RPTPβ protein throughout the first 2 weeks postlesion, IHC analysis of hippocampal RPTPβ revealed the strongest ML labeling at 7d postlesion, the period of robust terminal sprouting and synaptic reorganization (Figure 2 C,D). Although the RPTPβ antibody recognizes both full length and sRPTPβ, the absence of full length RPTPβ signal in our Western blots suggest that our IHC signal represents primarily sRPTPβ. In this case, we found punctate RPTPβ staining over the entire dentate ML (**contralateral distribution shown in** Figure 2 C), which was visibly increased in intensity on the ipsilateral deafferented side (Figure 2 D). When phosphacan was localized with ultrastructural ICC, we observed signal in both granule cell bodies and dendrites, consistent with the distribution of these isoforms seen by confocal IHC (data not shown).

To further investigate whether reactive astrocytes express phosphacan or RPTPβ after UEC, we also performed co-localization experiments where antibody for each splice variant was paired with GFAP antibody (Figure 2). No phosphacan or RPTPβ immunostaining was found within the cell bodies and major processes of ML astrocytes when examined with projected z stack images (**arrows in** Figures 2 E,F; **astrocytes identified by yellow arrows shown at higher magnification within insets**). These results suggest that neurons, not astrocytes, are the predominant source for phosphacan proteoglycans within the deafferented dentate gyrus.

Because the punctate confocal distribution of RPTPβ suggested synaptic localization, we also performed double label confocal IHC for RPTPβ and the post-synaptic density marker PSD-95 at 7d after UEC. A subset of RPTPβ positive puncta were found adjacent to sites stained with PSD-95 (**arrows in** Figures 3 A, B), suggesting contiguous distribution of the two proteins. Moreover, the relative density and size of RPTPβ puncta appeared greater in the ipsilateral deafferented ML (Figure 3 B) when compared with the contralateral side (Figure 3 A). In order to further investigate whether this pattern might represent pre- or post-synaptic localization of RPTPβ, we performed ultrastructural ICC on parallel 7d cases. Here RPTPβ was found predominantly within dendrites (**asterisk in** Figure 3 C), as well as in spines and adjacent to post-synaptic profiles (**arrowheads, arrows in** Figure 3 C **inset**). In some synaptic junctions, we also found evidence for RPTPβ label near vesicles within pre-synaptic terminals (**open arrow in** Figure 3C **inset**), a pattern similar to that observed by Hayashi and colleagues in embryonic cortical cells (2005).

Expression of Phosphacan and RPTPβ mRNA After UEC

Specific mRNA levels of phosphacan, full length RPTPβ, and sRPTPβ were measured in ipsilateral deafferented and contralateral control hippocampus at 2, 7, and 15d post lesion using qRT-PCR. We elected to express our qRT-PCR results relative total RNA input (Figure 4) because of two prior observations. First, we have shown low sample variance when these proteoglycans are normalized to total RNA (Harris et. al., 2009) and second, with the <2 fold changes in mRNA we observed, normalization to total RNA mass may be the most accurate approach for standardization of gene expression (Tricarico et al., 2002;Meldgaard et al., 2006). Phosphacan mRNA was increased only at 7d (113.6± 8.7%,

p<0.05). By contrast, elevations at both 2 and 15d postlesion for full length RPTPβ mRNA (122.8 ± 5.3% and 122.6 ± 7.8%; p<0.001) were found, while sRPTPβ mRNA was elevated at all three time points (111.7 ± 10.0% and 112.8 ± 5.6% for 2 and 7d, p<0.05; 118.8 ± 6.9% for 15d, p<0.01). Interestingly, the 2–15d increase in sRPTPβ transcript was consistent with time course of injury-induced elevations sRPTPβ protein (**see again** Figure 1 B). On the other hand, the 7d increase in hippocampal phosphacan mRNA was not correlated with increased phosphacan protein (see again Figure 1A). While expressed protein ultimately affects phenotype, changes in mRNA may independently reflect a biological response to cell perturbation. Examples of mismatch between transcript and protein expression are well documented (Mehra et al. 2003). We next investigated whether the observed differences between hippocampal phosphacan transcript and protein might be explained by subregional differences in protein distribution after lesion and our tissue sampling method.

Local Increase of Phosphacan in the Deafferented Molecular Layer

The time course profiles for phosphacan and RPTPβ were determined from whole hippocampal extracts, which could potentially dilute injury effects specific to the deafferented ML. In fact, our IHC results suggest that, with time after UEC, phosphacan was reduced over the granule cell layer and increased in the ipsilateral deafferented ML. Thus, we re-examined phosphacan protein level in Western blots at both 2 and 7d postlesion using ML/GCL enriched samples. At 7d, when qRT-PCR showed elevated transcript, but no increase in whole hippocampal phosphacan, tissue samples enriched in the deafferented ML revealed a significant increase in phosphacan protein (129.9±4.9%; p<0.05; Figure 5). Further, we also found that phosphacan was not increased in 2d ML enriched samples (**see again** Figure 1 A), consistent with the absence of significant rise in hippocampal phosphacan mRNA at this time. These results are supported by the fact that, despite a predominant shift in phosphacan from granule cell layer to ML at 2d, overall tissue signal for phosphacan was similar ipsilateral and contralateral to UEC lesion (**see again** Figure 2 A, B).

Discussion

The present study provides new detail regarding the expression of extracellular phosphacan and the transmembrane tyrosine phosphatases RPTPβ and sRPTPβ during the time course of reactive synaptogenesis. Overall, whole hippocampal phosphacan showed increased mRNA and protein expression during presynaptic degeneration and terminal sprouting, while the membrane bound sRPTPβ transcript and protein were elevated throughout the process of synaptogenesis. Lesion effects on full length RPTPβ were limited to elevated mRNA at 2 and 15d. Notably, whole hippocampal sRPTPβ had a correlated rise in both transcript and protein, while phosphacan and full length RPTPβ did not. Samples enriched in the deafferented ML showed a local dendritic 7d elevation in phosphacan protein, not detectable in whole hippocampal extracts, and ultrastructural ICC confirmed RPTPβ localization within ML dendrites and spines. Confocal dual label experiments indicated a close association between RPTPβ and PSD-95, consistent with the ultrastructural RPTPβ distribution, and showed that reactive astrocytes are not the primary source of phosphacan or RPTPβ in the deafferented zone. These results suggest that expression of different phosphacan splice variants is correlated with different phases of reactive synaptogenesis and that post-synaptic proteins may be principal targets of the membrane bound tyrosine phosphatase during synapse reconstruction.

Phosphacan and Reactive Synaptogenesis

Prior investigations have documented temporal shifts in the expression of phosphacan protein after UEC. Deller and colleagues (1997) first reported an increase in phosphacan

immunolabeling within the deafferented zone 6d after UEC, the period where collateral sprouting and synapse formation is initiated. Our IHC results show a similar pattern of increased phosphacan expression, however, we also observed phosphacan staining in granule cell somata of the contralateral dentate gyrus at 2d postlesion, a pattern which was shifted to predominant distribution over the deafferented outer ML on the lesioned side. At 7d postlesion, the same regional shift in phosphacan protein was visible and granule cell signal intensity was reduced. Differences in phosphacan profile between the present study and that of Deller et al. may be due to antibody specificity. It is possible that 3F8 antibody recognition of the phosphacan protein core revealed patterns of tissue distribution not recognized with the DSD-1-PG IgM antibody used in the earlier report.

Dual label confocal imaging failed to show phosphacan within ML reactive astrocytes, either at 2 or 7d after lesion. Differing levels of reactive gliosis across injury models could play a role since reactive astrocytes alter their phosphacan expression after certain types of experimental brain injury. For example, astrocytic expression of phosphacan is enhanced following spinal cord contusion (Vitellaro-Zuccarello et al., 2008), ischemic brain injury (Beck et al., 2008), and filter implant-induced glial scarring (McKeon et al., 1999). Notably, the attenuation of astroglial response to spinal cord contusion reversed the injury-induced rise in phosphacan, while elevated expression of other CSPGs (e.g. versican, neurocan, and brevican) remained unaltered (Vitellaro-Zuccarello et al., 2008). In contrast, our results suggest that UEC does not induce astrocyte production of phosphacan, but rather granule cells are a principal source of phosphacan after lesion and facilitate its redistribution to areas undergoing reactive synaptogenesis. This interpretation is consistent with prior observations by Okamoto and colleagues (2001) which show that phosphacan is not co-localized to astrocytes within adult hippocampus.

We also found that significant increase in phosphacan transcript was correlated with the onset of sprouting and synaptogenesis at 7d postlesion. An earlier study employing UEC in combination with fimbria/fornix lesion reported increased phosphacan mRNA, however only the 20d postinjury interval was sampled (Snyder et al., 1996). Here we failed to observe a change in phosphacan transcript as late as 15d, but since we did not sample the 20d time point, it remains possible that UEC produces elevation of phosphacan message at both 7 and 20d. Alternatively, the more severe combined insult used by Snyder and colleagues may have produced a longer lasting effect on phosphacan transcription. A second, more recent report applied precise laser dissection methods to isolate the outer deafferented dentate ML following UEC, assessing transcript expression for a panel of CSPGs including phosphacan (Schafer et al., 2008). Using qRT-PCR, this group found no significant change in phosphacan mRNA between 6h and 14d postlesion, including the 7d time point where we report increase in whole hippocampal transcript for phosphacan. These differences could be explained in at least two ways. First, our whole hippocampal extracts used for qRT-PCR contained granule neurons which, based upon IHC results, contribute significantly to phosphacan transcript. The laser dissected samples did not include dentate granule cell laminae. Second, the Schafer et al. study used 18S rRNA as a qRT-PCR reference gene, which we recently reported to be highly variable in expression and altered over time following UEC (Harris JL et al., 2009). Normalization of transcript to 18S rRNA could eliminate detection of experimental effect for specific genes of interest.

In contrast to IHC, Western blot analysis of whole hippocampal extracts failed to show a change in phosphacan protein 7d after UEC, the time point where whole hippocampal phosphacan transcript was elevated. This apparent asynchrony between mRNA and protein response to UEC reiterates the fact that transcript may not always predict protein content. Prior investigations have advised caution in interpreting proteoglycan expression after CNS trauma, particularly where mRNA quantification is the sole endpoint (Iaci et al. 2007). In the

present study, several conditions might account for this asynchrony. Postinjury pathology at 7d could suppress hippocampal translation of phosphacan mRNA. Alternatively, newly translated phosphacan protein might be rapidly degraded through the activation of extracellular matrix metalloproteinases which cleave phosphacan (Muir et al. 2002) and are upregulated in the hippocampus after UEC (Falo et al. 2006). The tPA/plasmin proteolytic pathway could also affect phosphacan during reactive synaptogenesis since plasmin degrades hypothalamic phosphacan during physiologically induced synaptic plasticity (Miyata et al 2005). Finally, our analysis of phosphacan in subregional tissue extracts suggests that sampling method may best explain the 7d transcript/protein mismatch. In contrast to the whole hippocampus, ML/GCL enriched tissue samples exhibited a 7d increase in phosphacan protein, consistent with the 7d elevation of phosphacan mRNA.

This 7d increase in phosphacan protein represents a local dentate response related to the postinjury period when sprouting and synapse formation is initiated. It is well established that endogenous growth factors can promote such sprouting in the injured CNS (Nieto-Sampedro & Bovolenta, 1990; Cui 2006; Deller et al., 2006). Phosphacan binds to a many of these growth factors, including basic fibroblast growth factor (FGF-2), pleiotrophin, amphoterin, and midkine (Milev et al., 1998a; Milev et al., 1998b; Maeda et al., 1999). This binding may localize these molecules at sites of sprouting, or sequester them for later mobilization. Increased phosphacan within the ML/GCL enriched sample is also consistent with the shift in the protein to the outer ML seen with IHC. When these results are considered with those of the Schafer et al. study, a clearer picture of phosphacan response to UEC emerges. We posit that deafferentation increases granule cell transcription of the phosphacan splice variant, producing protein which is transported distally along dendrites to ML sites of synaptic reorganization. Future PCR studies which assess local ML/GCL changes in transcript, as well as in situ hybridization experiments to confirm cell sources of phosphacan mRNA will be necessary to test this possibility.

RPTPβ and Reactive Synaptogenesis

Relative to phosphacan and other extracellular proteoglycans, there are fewer studies describing RPTPβ after CNS injury. Dobbertin and colleagues (2003) examined the expression of both receptor variants after cortical stab injury, where sRPTPβ protein and transcript did not change, but full length RPTPβ mRNA was reduced. A stab injury produces discrete tissue damage, local blood-brain barrier disruption, and astroglial scarring, with notably less compensatory plasticity. If sRPTPβ is more specifically supportive of synaptic remodeling, then no change in sRPTPβ expression would be predicted after focal stab insult. By contrast, sclerotic hippocampi from epileptic patients exhibited increase in RPTPβ immunoreactivity, primarily associated with gliosis and mossy fiber sprouting in the inner ML (Perosa et al. 2002). Similar to temporal lobe epilepsy, UEC induces axonal sprouting in the hippocampus. Here we also observed an elevation in RPTPβ protein, which persisted throughout the 15d postinjury period. Since full length RPTPβ is primarily a developmental isoform (Sakurai et al. 1996; Dobbertin et al 2003), and we failed to detect measurable amounts of that form by Western blot analysis, we conclude that our anti-RPTPβ IHC signal represents primarily sRPTPβ. Thus, the punctate outer ML distribution of sRPTPβ at 7d supports its interaction with the local environment to induce collateral sprouting and promote reorganization of postsynaptic dendrites. Indeed, our ultrastructural ICC studies confirmed localization of sRPTPβ within ML postsynaptic spines and dendrites, a pattern also reported by others for pyramidal neurons in cortex and hippocampus (Miyata et al., 2004; Hayashi et al., 2005).

In parallel confocal experiments, we found that ML sRPTPβ was often localized adjacent to PSD-95 signal, suggesting that it is positioned near reorganizing postsynaptic sites to influence protein phosphorylation. A similar RPTPβ distribution along Purkinje cell

dendritic shafts and somatic membranes was reported by Fukazawa et al. (2008). This localization suggests sRPTPβ effects on the distribution of synaptic proteins, possibly through their phosphorylation-directed positioning within the neuronal membrane (Kawachi et al., 1999; Fukazawa et al., 2008; Tezuka et al., 1999). Of these sRPTPβ targets, at least two, ErbB4 (Erlich et al., 2000) and PSD-95 (Ansari et al., 2008), show a change in expression after traumatic brain injury. A similar role for RPTPβ was described during morphogenesis of cerebellar Purkinje dendrites *in vitro*, where RPTPβ inhibition produced aberrant dendritic structure (Tanaka et al., 2003). Again, it appears that the actions of this splice variant are mediated through neuronal populations, as little evidence of significant astrocytic sRPTPβ was observed.

Concurrent elevations in sRPTPβ mRNA were also found throughout the time course of UEC induced synaptogenesis. Persistent elevation suggests that the protein product of this splice variant influences all phases of the synaptogenic process. Using the same UEC/FFX lesion model as for their phosphacan analysis, Snyder and colleagues (1996) reported an increase in RPTPβ mRNA at 20d postinjury. In the present study, we also found increased RPTPβ transcript at 15d after UEC lesion alone, suggesting that a single deafferentation insult is sufficient to up-regulate transmembrane phosphacan genes during the later stages of reactive synaptogenesis. Interestingly, message for full length RPTPβ did increase at 2d and 15d postlesion. However, since we could not detect this form with immunoblots, elevated transcript may represent the accumulation of stable, but untranslated mRNA. Using a cortical knife lesion model, Dobbertin and colleagues (2003) also report an acute postinjury shift in full length RPTPβ transcript without detectable full length protein in their tissue extracts. Since expression of the full length isoform has been best described during embryological development (Sakurai et al. 1996) and UEC deafferentation induces synaptogenesis similar to that observed in the developing hippocampus, it is plausible that full length RPTPβ also participates in synaptic reorganization after injury. Nevertheless, additional studies using more specific markers of RPTPβ splice variants will be required to clarify the role of the full length isoform.

Complexity of Phosphacan and RPTPβ Response After Brain Injury

While many CSPGs such as aggrecan (Schafer et al., 2008), neurocan (Asher et al., 2000; Schafer et al., 2008), brevican (Schafer et al., 2008), versican (Asher et al., 2002), and NG2 (Tang et al., 2003; Schafer et al., 2008) are up-regulated after CNS injury, phosphacan response may be mixed depending upon injury modality and survival interval sampled (Matsui et al., 2002; Dobbertin et al., 2003; Okamoto et al., 2003; Jones et al., 2003; Tang et al., 2003; Heck et al., 2004). In some cases, both increases and decreases in phosphacan occur concurrently within different sub-regions after injury. For example, phosphacan is reduced at the core but increased at the margin of spinal cord lesion (Tang et al., 2003), while it may be increased at the border of stroke infarct, but decreased in the peri-infarct tissue (Carmichael et al., 2005).

This complex reaction pattern appears most related to the type of injury induced, extent of synaptic plasticity involved, and the postinjury time frame examined. When the injury site is physically separated from the deafferented region, as occurs with UEC lesion, necrotic cell death and glial scarring do not directly affect the adaptive synaptic plasticity processes (Deller et al., 2000). These differences would explain a differential phosphacan response relative to other published models, which may depend upon the extent of neuronal and glial cell loss in the areas examined and the survival intervals targeted (Jones et al., 2003; Tang et al., 2003). Alternatively, loss of neuronal activity by massive deafferentation in the UEC model could shift expression of proteins whose transcription is regulated by such activity. Here, the loss of perforant path input profoundly reduces synaptic drive, resulting in extensive plasticity and pronounced effects on phosphacan/RPTPβ during each phase of

reactive synaptogenesis. Interestingly, an inverse relationship between cell activity and phosphacan/RPTPβ expression has been reported in supraoptic magnocellular neurons (Miyata et al., 2004), supporting the idea that change in neuronal activity may also affect proteoglycan expression following UEC deafferentation. Future studies employing pharmacological inactivation of the entorhinal cortex or septal formation may determine the extent to which aberrant neuronal activity regulates proteoglycan function during synaptic reorganization in the hippocampus.

Conclusions

In summary, the data presented here provide new evidence that phosphacan and sRPTPβ each play a role in the reactive synaptic plasticity that occurs after brain injury. These two splice variants are differentially elevated during reactive synaptogenesis induced by UEC lesion. Shifts in phosphacan expression appear more specifically associated with the period of sprouting and synapse reconstruction, while transmembrane RPTPβ is activated throughout the period of synapse morphogenesis and stabilization. These changes appear to be primarily associated with neurons and likely contribute to adaptive recovery after brain insult. In order to promote better recovery after brain injury, we must continue to explore how ECM proteins affect the local environment during synaptogenesis. Such studies will help to define differences between injuries where recovery is successful and those where recovery fails.

Acknowledgments

The authors gratefully acknowledge the expert technical assistance of Lesley Harris, Raiford Black and Nancy Lee. This study was supported by NIH research grants NS-044372 (LLP), NS-057758 (TMR) and a Virginia Commonwealth Neurotrauma Initiative Award 07-302F (TMR). All qRT-PCR was conducted at the Nucleic Acids Research Facilities, Center for the Study of Biological Complexity, Virginia Commonwealth University. Microscopy was performed at the Virginia Commonwealth University Department of Anatomy and Neurobiology Microscopy Facility, supported, in part, with funding from NIH-NINDS Center P30 core grant NS-047463.

References

Ansari MA, Roberts KN, Scheff SW. A time course of contusion-induced oxidative stress and synaptic proteins in cortex in a rat model of TBI. J Neurotrauma. 2008; 25:513–526. [PubMed: 18533843]

Asher RA, Morgenstern DA, Fidler PS, Adcock KH, Oohira A, Braistead JE, Levine JM, Margolis RU, Rogers JH, Fawcett JW. Neurocan is upregulated in injured brain and in cytokine-treated astrocytes. J Neurosci. 2000; 20:2427–2438. [PubMed: 10729323]

Asher RA, Morgenstern DA, Shearer MC, Adcock KH, Pesheva P, Fawcett JW. Versican is upregulated in CNS injury and is a product of oligodendrocyte lineage cells. J Neurosci. 2002; 22:2225–2236. [PubMed: 11896162]

Beck H, Semisch M, Culmsee C, Plesnila N, Hatzopoulos AK. Egr-1 regulates expression of the glial scar component phosphacan in astrocytes after experimental stroke. Am J Pathol. 2008; 173:77–92. [PubMed: 18556777]

Bicknese AR, Sheppard AM, O'Leary DD, Pearlman AL. Thalamocortical axons extend along a chondroitin sulfate proteoglycan-enriched pathway coincident with the neocortical subplate and distinct from the efferent path. J Neurosci. 1994; 14:3500–3510. [PubMed: 8207468]

Bradbury EJ, Moon LD, Popat RJ, King VR, Bennett GS, Patel PN, Fawcett JW, McMahon SB. Chondroitinase ABC promotes functional recovery after spinal cord injury. Nature. 2002; 416:636–640. [PubMed: 11948352]

Carmichael ST, Archibeque I, Luke L, Nolan T, Momiy J, Li S. Growth-associated gene expression after stroke: Evidence for a growth-promoting region in peri-infarct cortex. Exp Neurol. 2005; 193:291–311. [PubMed: 15869933]

Cui Q. Actions of neurotrophic factors and their signaling pathways in neuronal survival and axonal regeneration. Mol Neurobiol. 2006; 33:155–179. [PubMed: 16603794]

Davies SJ, Goucher DR, Doller C, Silver J. Robust regeneration of adult sensory axons in degenerating white matter of the adult rat spinal cord. J Neurosci. 1999; 19:5810–5822. [PubMed: 10407022]

Deller T, Haas CA, Naumann T, Joester A, Faissner A, Frotscher M. Up-regulation of astrocyte-derived tenascin-C correlates with neurite outgrowth in the rat dentate gyrus after unilateral entorhinal cortex lesion. Neuroscience. 1997; 81:829–846. [PubMed: 9316032]

Deller T, Haas CA, Frotscher M. Reorganization of the rat fascia dentata after a unilateral entorhinal cortex lesion. role of the extracellular matrix. Ann N Y Acad Sci. 2000; 911:207–220. [PubMed: 10911876]

Deller T, Haas CA, Freiman TM, Phinney A, Jucker M, Frotscher M. Lesion-induced axonal sprouting in the central nervous system. Adv Exp Med Biol. 2006; 557:101–121. [PubMed: 16955706]

Dobbertin A, Rhodes KE, Garwood J, Properzi F, Heck N, Rogers JH, Fawcett JW, Faissner A. Regulation of RPTPbeta/phosphacan expression and glycosaminoglycan epitopes in injured brain and cytokine-treated glia. Mol Cell Neurosci. 2003; 24:951–971. [PubMed: 14697661]

Erlich S, Shohami E, Pinkas-Kramarski R. Closed head injury induces up-regulation of ErbB-4 receptor at the site of injury. Mol Cell Neurosci. 2000; 16:597–608. [PubMed: 11083921]

Faissner A, Clement A, Lochter A, Streit A, Mandl C, Schachner M. Isolation of a neural chondroitin sulfate proteoglycan with neurite outgrowth promoting properties. J Cell Biol. 1994; 126:783–799. [PubMed: 7519189]

Falo MC, Fillmore HL, Reeves TM, Phillips LL. Matrix metalloproteinase-3 expression profile differentiates adaptive and maladaptive synaptic plasticity induced by traumatic brain injury. J Neurosci Res. 2006; 84:768–781. [PubMed: 16862547]

Fukazawa N, Yokoyama S, Eiraku M, Kengaku M, Maeda N. Receptor type protein tyrosine phosphatase zeta-pleiotrophin signaling controls endocytic trafficking of DNER that regulates neuritogenesis. Mol Cell Biol. 2008; 28:4494–4506. [PubMed: 18474614]

Garwood J, Schnadelbach O, Clement A, Schutte K, Bach A, Faissner A. DSD-1- proteoglycan is the mouse homolog of phosphacan and displays opposing effects on neurite outgrowth dependent on neuronal lineage. J Neurosci. 1999; 19:3888–3899. [PubMed: 10234020]

Grumet M, Flaccus A, Margolis RU. Functional characterization of chondroitin sulfate proteoglycans of brain: Interactions with neurons and neural cell adhesion molecules. J Cell Biol. 1993; 120:815–824. [PubMed: 8425902]

Harris JL, Reeves TM, Phillips LL. Injury modality, survival interval and sample region are critical determinants of qRT-PCR reference gene selection during long-term recovery from brain trauma. J Neurotrauma. 2009; 26:1–13. [PubMed: 19196178]

Harris NG, Carmichael ST, Hovda DA, Sutton RL. Traumatic brain injury results in disparate regions of chondroitin sulfate proteoglycan expression that are temporally limited. J Neurosci Res. 2009; 87:2937–2950. [PubMed: 19437549]

Hayashi N, Oohira A, Miyata S. Synaptic localization of receptor-type protein tyrosine phosphatase zeta/beta in the cerebral and hippocampal neurons of adult rats. Brain Res. 2005; 1050:163–169. [PubMed: 15982644]

Heck N, Garwood J, Loeffler JP, Larmet Y, Faissner A. Differential upregulation of extracellular matrix molecules associated with the appearance of granule cell dispersion and mossy fiber sprouting during epileptogenesis in a murine model of temporal lobe epilepsy. Neuroscience. 2004; 129:309–324. [PubMed: 15501589]

Huang WC, Kuo WC, Cherng JH, Hsu SH, Chen PR, Huang SH, Huang MC, Liu JC, Cheng H. Chondroitinase ABC promotes axonal re-growth and behavior recovery in spinal cord injury. Biochem Biophys Res Commun. 2006; 349:963–968. [PubMed: 16965762]

Iaci JF, Vecchione AM, Zimber MP, Caggiano AO. Chondroitin sulfate proteoglycans in spinal cord contusion injury and the effects of chondroitinase treatment. J Neurotrauma. 2007; 24:1743–1759. [PubMed: 18001203]

Jones LL, Margolis RU, Tuszynski MH. The chondroitin sulfate proteoglycans neurocan, brevican, phosphacan, and versican are differentially regulated following spinal cord injury. Exp Neurol. 2003; 182:399–411. [PubMed: 12895450]

Kawachi H, Tamura H, Watakabe I, Shintani T, Maeda N, Noda M. Protein tyrosine phosphatase zeta/RPTPbeta interacts with PSD-95/SAP90 family. Brain Res Mol Brain Res. 1999; 72:47–54. [PubMed: 10521598]

Keppel, G. Design and Analysis: A Researcher's Hand book. Englewood Cliffs, NJ: Prentice Hall; 1991.

Levine, G. A Guide to SPSS for Analysis of Variance. Hillsdale, NJ: Lawrence-Erlbaum, Assocates; 1991.

Levy JB, Canoll PD, Silvennoinen O, Barnea G, Morse B, Honegger AM, Huang JT, Cannizzaro LA, Park SH, Druck T. The cloning of a receptor-type protein tyrosine phosphatase expressed in the central nervous system. J Biol Chem. 1993; 268:10573–10581. [PubMed: 8387522]

Loesche J, Steward O. Behavioral correlates of denervation and reinnervation of the hippocampal formation of the rat: Recovery of alternation performance following unilateral entorhinal cortex lesions. Brain Res Bull. 1977; 2:31–39. [PubMed: 861769]

Maeda N, Ichihara-Tanaka K, Kimura T, Kadomatsu K, Muramatsu T, Noda M. A receptor-like protein-tyrosine phosphatase PTPzeta/RPTPbeta binds a heparin-binding growth factor midkine. involvement of arginine 78 of midkine in the high affinity binding to PTPzeta. J Biol Chem. 1999; 274:12474–12479. [PubMed: 10212223]

Matsui F, Kawashima S, Shuo T, Yamauchi S, Tokita Y, Aono S, Keino H, Oohira A. Transient expression of juvenile-type neurocan by reactive astrocytes in adult rat brains injured by kainate-induced seizures as well as surgical incision. Neuroscience. 2002; 112:773–781. [PubMed: 12088737]

Maurel P, Rauch U, Flad M, Margolis RK, Margolis RU. Phosphacan, a chondroitin sulfate proteoglycan of brain that interacts with neurons and neural cell-adhesion molecules, is an extracellular variant of a receptor-type protein tyrosine phosphatase. Proc Natl Acad Sci U S A. 1994; 91:2512–2516. [PubMed: 7511813]

Mehra A, Lee KH, Hatzimanikatis V. Insights into the relation between mRNA and protein expression patterns I: Theoretical considerations. Biotechnol Bioeng. 2003; 84:822–833. [PubMed: 14708123]

McKeon RJ, Jurynec MJ, Buck CR. The chondroitin sulfate proteoglycans neurocan and phosphacan are expressed by reactive astrocytes in the chronic CNS glial scar. J Neurosci. 1999; 19:10778–10788. [PubMed: 10594061]

Meldgaard M, Fenger C, Lambertsen KL, Pedersen MD, Ladeby R, Finsen B. Validation of two reference genes for mRNA level studies of murine disease models in neurobiology. J Neurosci Methods. 2006; 156:101–110. [PubMed: 16554095]

Meng K, Rodriguez-Pena A, Dimitrov T, Chen W, Yamin M, Noda M, Deuel TF. Pleiotrophin signals increased tyrosine phosphorylation of beta beta-catenin through inactivation of the intrinsic catalytic activity of the receptor-type protein tyrosine phosphatase beta/zeta. Proc Natl Acad Sci U S A. 2000; 97:2603–2608. [PubMed: 10706604]

Milev P, Monnerie H, Popp S, Margolis RK, Margolis RU. The core protein of the chondroitin sulfate proteoglycan phosphacan is a high-affinity ligand of fibroblast growth factor-2 and potentiates its mitogenic activity. J Biol Chem. 1998a; 273:21439–21442. [PubMed: 9705269]

Milev P, Chiba A, Haring M, Rauvala H, Schachner M, Ranscht B, Margolis RK, Margolis RU. High affinity binding and overlapping localization of neurocan and phosphacan/proteintyrosine phosphatase-zeta/beta with tenascin-R, amphoterin, and the heparin-binding growth-associated molecule. J Biol Chem. 1998b; 273:6998–7005. [PubMed: 9507007]

Miyata S, Akagi A, Hayashi N, Watanabe K, Oohira A. Activity-dependent regulation of a chondroitin sulfate proteoglycan 6B4 phosphacan/RPTPbeta in the hypothalamic supraoptic nucleus. Brain Res. 2004; 1017:163–171. [PubMed: 15261112]

Moon LD, Asher RA, Rhodes KE, Fawcett JW. Regeneration of CNS axons back to their target following treatment of adult rat brain with chondroitinase ABC. Nat Neurosci. 2001; 4:465–466. [PubMed: 11319553]

Morgenstern DA, Asher RA, Fawcett JW. Chondroitin sulphate proteoglycans in the CNS injury response. Prog Brain Res. 2002; 137:313–332. [PubMed: 12440375]

Muir EM, Adcock KH, Morgenstern DA, Clayton R, von Stillfried N, Rhodes K, Ellis C, Fawcett JW, Rogers JH. Matrix metalloproteases and their inhibitors are produced by overlapping populations of activated astrocytes. Brain Res Mol Brain Res. 2002; 100:103–117. [PubMed: 12008026]

Nieto-Sampedro M, Bovolenta P. Growth factors and growth factor receptors in the hippocampus. role in plasticity and response to injury. Prog Brain Res. 1990; 83:341–355. [PubMed: 2168060]

Niisato K, Fujikawa A, Komai S, Shintani T, Watanabe E, Sakaguchi G, Katsuura G, Manabe T, Noda M. Age-dependent enhancement of hippocampal long-term potentiation and impairment of spatial learning through the rho-associated kinase pathway in protein tyrosine phosphatase receptor type Z-deficient mice. J Neurosci. 2005; 25:1081–1088. [PubMed: 15689543]

Okamoto M, Sakiyama J, Kurazono S, Mori S, Nakata Y, Nakaya N, Oohira A. Developmentally regulated expression of brain-specific chondroitin sulfated proteoglycans, neurocan and phosphacan, in the postnatal rat hippocampus. Cell Tissue Res. 2001; 306:217–229. [PubMed: 11702233]

Okamoto M, Sakiyama J, Mori S, Kurazono S, Usui S, Hasegawa M, Oohira A. Kainic acid-induced convulsions cause prolonged changes in the chondroitin sulfate proteoglycans neurocan and phosphacan in the limbic structures. Exp Neurol. 2003; 184:179–195. [PubMed: 14637091]

Oohira A, Matsui F, Katoh-Semba R. Inhibitory effects of brain chondroitin sulfate proteoglycans on neurite outgrowth from PC12D cells. J Neurosci. 1991; 11:822–827. [PubMed: 2002362]

Pariser H, Ezquerra L, Herradon G, Perez-Pinera P, Deuel TF. Fyn is a downstream target of the pleiotrophin/receptor protein tyrosine phosphatase beta/zeta-signaling pathway: Regulation of tyrosine phosphorylation of fyn by pleiotrophin. Biochem Biophys Res Commun. 2005; 332:664–669. [PubMed: 15925565]

Perosa SR, Porcionatto MA, Cukiert A, Martins JR, Passeroti CC, Amado D, Matas SL, Nader HB, Cavalheiro EA, Leite JP, Naffah-Mazzacoratti MG. Glycosaminoglycan levels and proteoglycan expression are altered in the hippocampus of patients with mesial temporal lobe epilepsy. Brain Res Bull. 2002; 58:509–516. [PubMed: 12242104]

Phillips LL, Lyeth BG, Hamm RJ, Povlishock JT. Combined fluid percussion brain injury and entorhinal cortical lesion: A model for assessing the interaction between neuroexcitation and deafferentation. J Neurotrauma. 1994; 11:641–656. [PubMed: 7723064]

Pizzorusso T, Medini P, Berardi N, Chierzi S, Fawcett JW, Maffei L. Reactivation of ocular dominance plasticity in the adult visual cortex. Science. 2002; 298:1248–1251. [PubMed: 12424383]

Properzi F, Asher RA, Fawcett JW. Chondroitin sulphate proteoglycans in the central nervous system: Changes and synthesis after injury. Biochem Soc Trans. 2003; 31:335–336. [PubMed: 12653631]

Sakurai T, Friedlander DR, Grumet M. Expression of polypeptide variants of receptor-type protein tyrosine phosphatase beta: The secreted form, phosphacan, increases dramatically during embryonic development and modulates glial cell behavior in vitro. J Neurosci Res. 1996; 43:694–706. [PubMed: 8984199]

Sakurai T, Lustig M, Nativ M, Hemperly JJ, Schlessinger J, Peles E, Grumet M. Induction of neurite outgrowth through contactin and nr-CAM by extracellular regions of glial receptor tyrosine phosphatase beta. J Cell Biol. 1997; 136:907–918. [PubMed: 9049255]

Schafer R, Dehn D, Burbach GJ, Deller T. Differential regulation of chondroitin sulfate proteoglycan mRNAs in the denervated rat fascia dentata after unilateral entorhinal cortex lesion. Neurosci Lett. 2008; 439:61–65. [PubMed: 18511192]

Snow DM, Lemmon V, Carrino DA, Caplan AI, Silver J. Sulfated proteoglycans in astroglial barriers inhibit neurite outgrowth in vitro. Exp Neurol. 1990; 109:111–130. [PubMed: 2141574]

Snyder SE, Li J, Schauwecker PE, McNeill TH, Salton SR. Comparison of RPTP zeta/beta, phosphacan, and trkB mRNA expression in the developing and adult rat nervous system and induction of RPTP zeta/beta and phosphacan mRNA following brain injury. Brain Res Mol Brain Res. 1996; 40:79–96. [PubMed: 8840016]

Steward O, Vinsant SL, Davis L. The process of reinnervation in the dentate gyrus of adult rats: An ultrastructural study of changes in presynaptic terminals as a result of sprouting. J Comp Neurol. 1988; 267:203–210. [PubMed: 3343397]

Tamura H, Fukada M, Fujikawa A, Noda M. Protein tyrosine phosphatase receptor type Z is involved in hippocampus-dependent memory formation through dephosphorylation at Y1105 on p190 RhoGAP. Neurosci Lett. 2006; 399:33–38. [PubMed: 16513268]

Tanaka M, Maeda N, Noda M, Marunouchi T. A chondroitin sulfate proteoglycan PTPzeta /RPTPbeta regulates the morphogenesis of purkinje cell dendrites in the developing cerebellum. J Neurosci. 2003; 23:2804–2814. [PubMed: 12684467]

Tang X, Davies JE, Davies SJ. Changes in distribution, cell associations, and protein expression levels of NG2, neurocan, phosphacan, brevican, versican V2, and tenascin-C during acute to chronic maturation of spinal cord scar tissue. J Neurosci Res. 2003; 71:427–444. [PubMed: 12526031]

Tezuka T, Umemori H, Akiyama T, Nakanishi S, Yamamoto T. PSD-95 promotes fynmediated tyrosine phosphorylation of the N-methyl-D-aspartate receptor subunit NR2A. Proc Natl Acad Sci U S A. 1999; 96:435–440. [PubMed: 9892651]

Tricarico C, Pinzani P, Bianchi S, Paglierani M, Distante V, Pazzagli M, Bustin SA, Orlando C. Quantitative real-time reverse transcription polymerase chain reaction: Normalization to rRNA or single housekeeping genes is inappropriate for human tissue biopsies. Anal Biochem. 2002; 309:293–300. [PubMed: 12413463]

Vitellaro-Zuccarello L, Mazzetti S, Madaschi L, Bosisio P, Fontana E, Gorio A, De Biasi S. Chronic erythropoietin-mediated effects on the expression of astrocyte markers in a rat model of contusive spinal cord injury. Neuroscience. 2008; 151:452–466. [PubMed: 18065151]

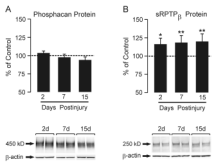

Figure 1. Time course of whole hippocampal phosphacan and RPTPβ protein expression at 2, 7 and 15d after UEC

Western blot for phosphacan (**A**) within the deafferented hippocampus showed no difference from control at any of the three time points. 2d and 15d n=6; 7d n=9. In (**B**), Western blot probe for RPTPβ (antibody recognizing both full length and short transmembrane phosphatase) showed a significant increase in protein within the deafferented hippocampus at all time points when compared with contralateral controls. Representative ipsilateral (left)/contralateral (right) gel pairs are illustrated below each time point. 2d and 15d n=6; 7d n=9; *p<0.02, **p<0.001.

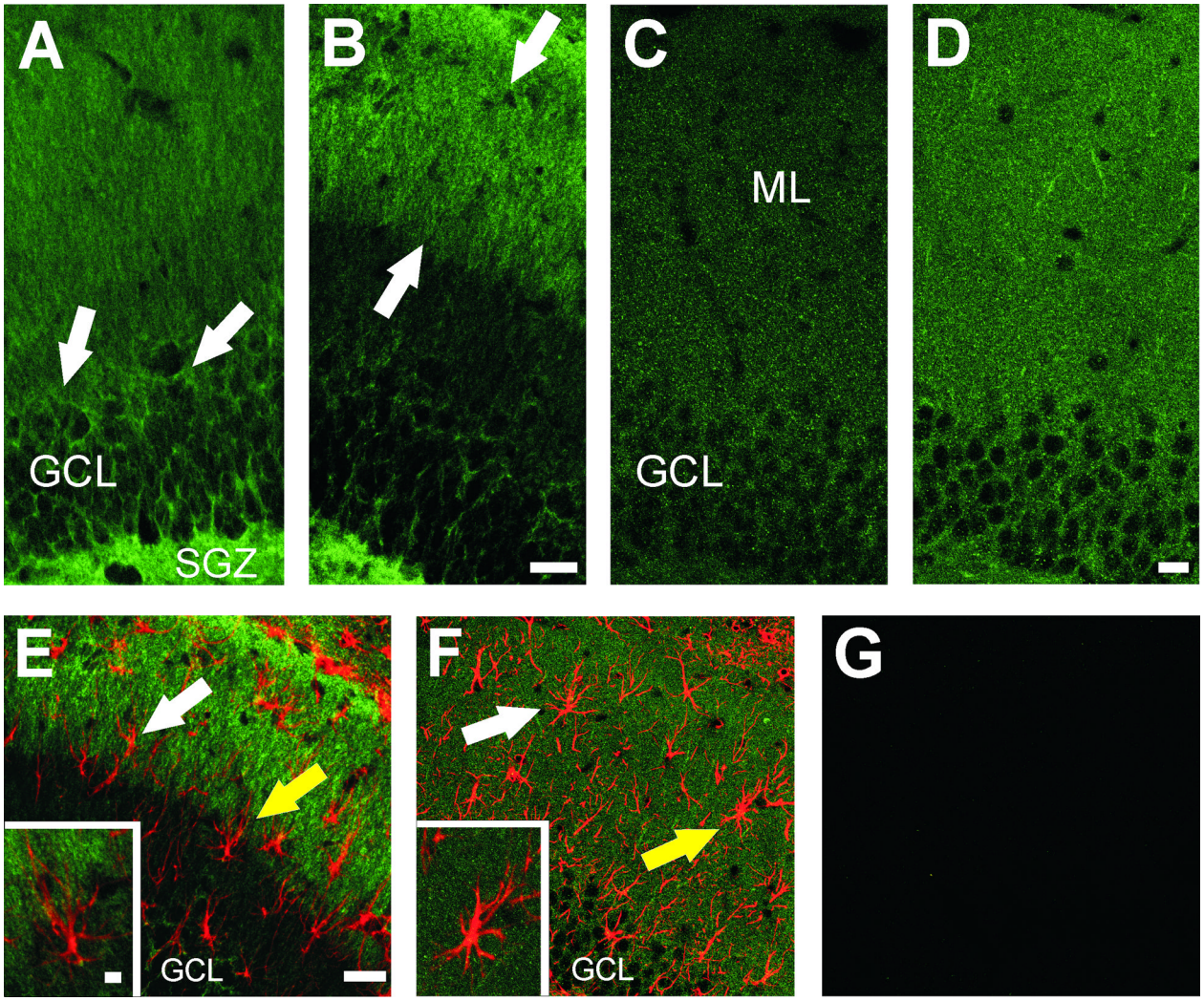

Figure 2. Localization of phosphacan and RPTPβ in deafferented dentate gyrus 2 and 7d after UEC

Projected z stack images show phosphacan (3F8) signal at 2d (**A, B**) shows predominant localization over the granule cell body layer (GCL) and subgranular zone (SGZ) of contralateral control (arrows in **A**). After lesion (**B**), phosphacan is increased in the outer molecular layer (OML, arrows) and decreased in the GCL and SGZ. By contrast, the distribution of RPTPβ at 7d post-lesion (**C, D**) is punctate and visible throughout the ML at higher density (**D**) than in the contralateral control (**C**). Confocal dual labeling of phosphacan at 2d (green in **E**) and RPTPβ at 7d (green in **F**) with astrocyte marker (GFAP, red) in the deafferented ML suggests that reactive astrocytes are not the principal source of either splice variant. The two markers fail to show significant overlap of signal (white arrows in panels **E,F**). Individual examples of reactive astrocytes (yellow arrows) are show enlarged in each inset. Minus primary controls had only low background signal (**G**). Bar in **A–D**=20μm; **E–G**=40μm; **insets**=5 μm.

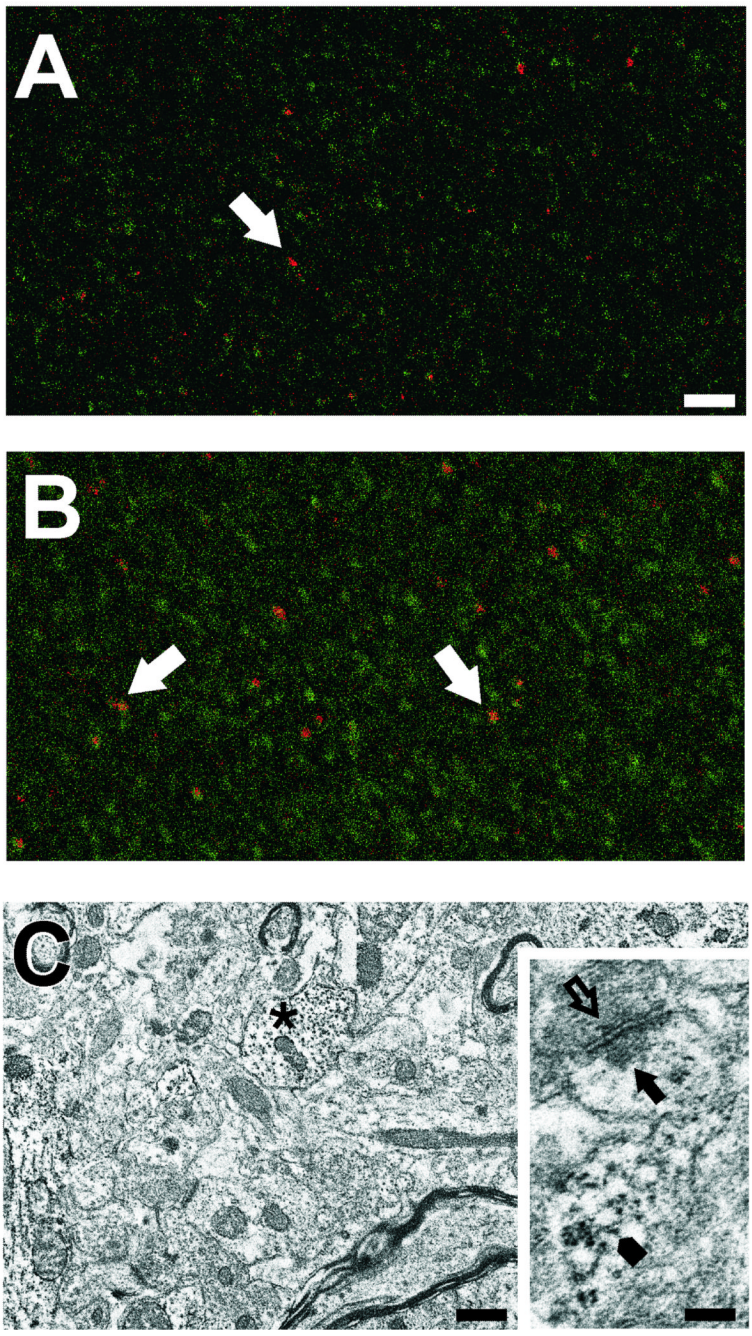

Figure 3. RPTPβ distribution in dentate ML at 7d after UEC lesion

Confocal IHC shows RPTPβ (green) at punctate sites in the outer contralateral ML (**A**). These sites are more numerous and of larger size in the deafferented ML (**B**), where RPTPβ is found adjacent to postsynaptic sites (PSD-95 positive profiles, red; arrows in **A,B**). Ultrastructural ICC shows RPTPβ localized in dendritic profiles (asterisk) in the outer ML of a contralateral hemisphere (**C**). Inset in **C** shows RPTPβ present in a spine (arrowhead), postsynaptic (arrow) and presynaptic (open arrow) sites from a section without counter stain. Bar in **A, B**=25μm; **C**=0.5μm; **inset**=0.2μm.

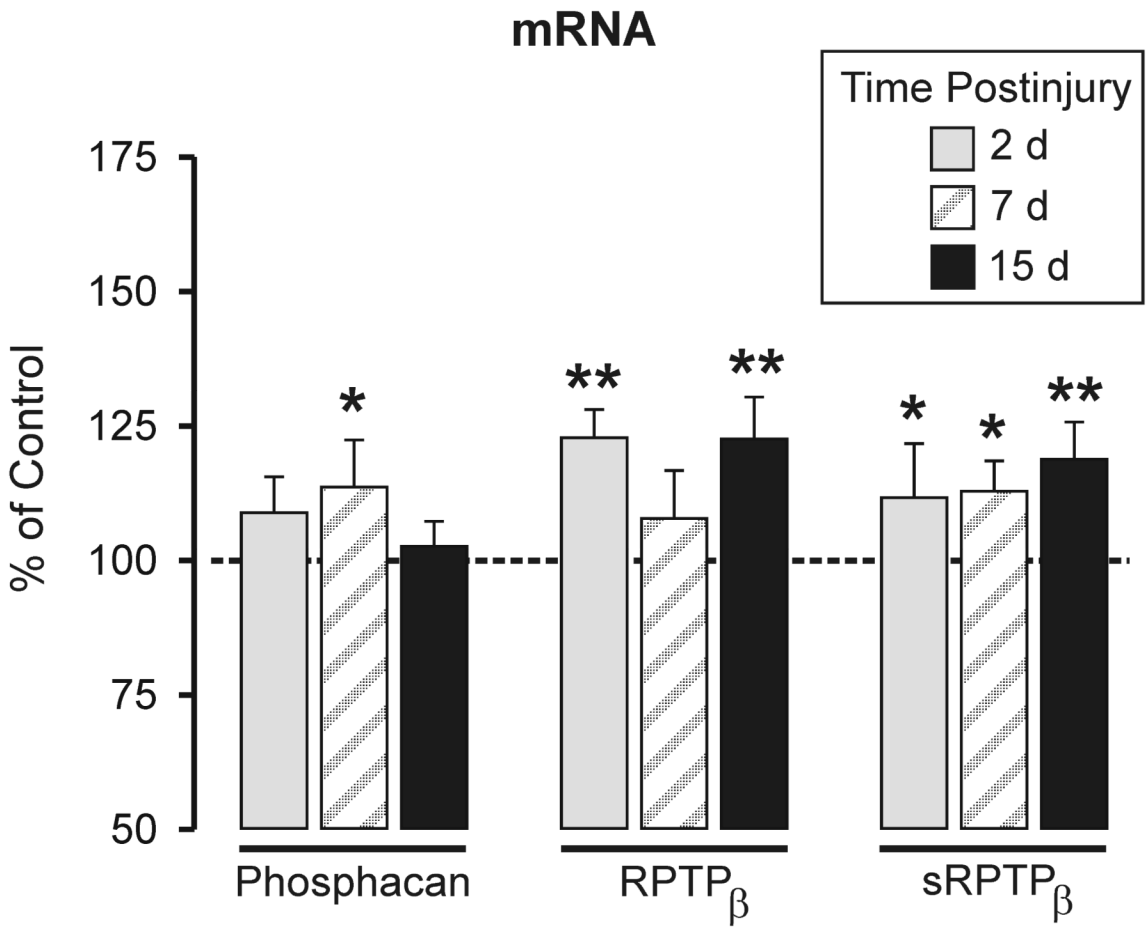

Figure 4. Quantitative RT-PCR analysis of hippocampal phosphacan, short and full length RPTPβ transcripts at 2, 7 and 15d after UEC lesion

Change in mRNA expression shown as percent of contralateral transcript level and normalized to total RNA input. Differences were detected between the three splice variants over time post-lesion. Phosphacan mRNA increased only at 7d post-lesion. The full length splice variant (RPTPβ) was increased at 2 and 15d, while sRPTPβ was elevated over all post-lesion intervals. 2d and 15d n=6; 7d n=5; *p<0.05, **p<0.01.

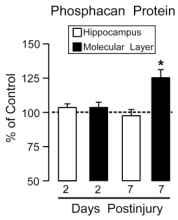

Figure 5. Phosphacan protein expression in the ML enriched samples from dentate gyrus at 2 and 7d following UEC lesion

Enriched ML extracts are compared with whole hippocampal data (re-plotted from Figure 1). At 2d, when whole hippocampal phosphacan is elevated, ML phosphacan did not change relative to control values. By contrast, the 7d ML enriched fraction showed increased phosphacan, positively correlated with elevation of hippocampal phosphacan transcript at 7d. 2d n=4; 7d n=3; *p<0.02.

Table 1

Primer pairs designed for qRT-PCR of RPTP splice variants and the housekeeping gene cyclophilin A.

gene	Oligo sequence
phosphacan forward	5’- GGGCATTCAGGAGTATCCAACA-3’
phosphacan reverse	5’- TCCGTGACTCTTCTATTTTTACTTTCAT-3’
phosphacan probe	5’- TCAGCACATCTCGTTCTATCCCTTTGCTCA-3’
RPTPβ forward	5’- GCAGAGGCCAGTAATAGTAGCCAT-3’
RPTPβ reverse	5’- TAGATGAGAATACCAACAAGAACCACTAG-3’
RPTPβ probe	5’- ACACGATCACAAGGGGTATAACCGCCTT-3’
sRPTPβ forward	5’-ACAATGAGGCCAGTAATAGTAGCCAT-3’
sRPTPβ reverse	5’- TAGATGAGAATACCAACAAGAACCACTAG -3’
sRPTPβ probe	5’- AGACACGATCACAAGGGGTATAACCGCCT -3’
cyclophilin A forward	5’- CTGTTTGCAGACAAAGTTCCAAA -3’
cyclophilin A reverse	5’- AGGAACCCTTATAGCCAAATCCTT -3'
cyclophilin A probe	5’- CAGCAGAAAACTTTCGTGCTCTGAGCACT -3'